

One-Step Synthesis of Porous Graphitic Carbon Nitride and the Photocatalytic Performance under Visible-Light Irradiation

Ligang Zhang^{*}, Naipeng Zhang, Dejin Zhang, Wenzhu Ouyang and Yong Xie^{*}

Anhui Key Laboratory of Spin Electron and Nanomaterials of Anhui Higher Education Institutes, School of Chemistry and Chemical Engineering, Suzhou University, Suzhou 234000, China

Abstract: Porous graphitic carbon nitride (pg-C₃N₄) was synthesized via a facile one-step dicyandiamide (DCDA) high-temperature calcination method using heat-labile ammonium bicarbonate (NH₄HCO₃) as the gaseous template, and different pg-C₃N₄ materials were obtained by mixing various mass ratios of NH₄HCO₃ into DCDA. The micro-structures and -morphologies of the porous materials were characterized by X-ray diffraction (XRD) and Scanning Electron Microscope (SEM) respectively, and the photocatalytic degradation of methylene blue (MB) dye was tested under visible-light irradiation. It is found that the thermal decomposition of NH₄HCO₃ promoted destruction of the layer-structured g-C₃N₄ and increment of the specific surface area, producing more porous structures on the material surfaces, which is considered to be vital for the improvement of photocatalytic performance. Compared with the photocatalyst calcined by pure DCDA, the pg-C₃N₄ photocatalysts obtained by mixing the two raw materials performed better on MB dye degradation. Moreover, photocatalytic efficiency of the catalysts improved significantly with increasing NH₄HCO₃ contents in the raw materials. The degradation rate photocatalyzed by pg-C₃N₄ materials can reach more than 90% within 1.5 h, 6.5 times higher than that of the control material. It comes up to 99% at 2 h, basically achieving the complete degradation and decolorization of MB dye.

Keywords: One-step synthesis, graphitic carbon nitride, porous structures, photocatalytic performance, visible-light irradiation.

1. INTRODUCTION

With the continuous development of industrial technology and society, the problems of energy shortage and environmental pollution and destruction have become increasingly prominent [1-4], attracting more and more attention. The excessive consumption of non-renewable energy such as coal, oil and natural gas makes the resources available less and less, and the environmental pollution caused by excessive consumption also troubles human production and life [5-7]. It is urgent to seek some effective solution.

Photocatalysis technology has been widely concerned by relevant researchers by virtue of its great potential in energy and environmental applications [8-10]. Since scientists in 1972 discovered TiO₂ electrodes on decomposing water under ultraviolet light [11], as a milestone it opened the prelude to the photocatalysis researches. Since then, a large number of materials with photocatalytic properties, such as cadmium sulfide [3-5, 12, 13], molybdenum disulfide [4, 14-16], boron nitride [6, 7, 17, 18], etc., have been widely studied and developed. Metal-free polymer semiconductor graphitic carbon nitride (g-C₃N₄) materials have been used in many research fields,

such as photocatalysis [10, 19-21], electrocatalysis [22-24] and fluorescence detection [25-27] because of their good biocompatibility, easy preparation, low cost, non-toxicity, good stability and visible-light excitation [2, 10, 19, 28]. The micro-structures of photocatalysts are closely related to their physico-chemical properties and photocatalytic performance [1, 2, 9, 23, 29]. However, bulk g-C₃N₄ possesses some inherent shortcomings, such as low specific surface area [20, 30], low utilization of visible-light [2, 29], and easy recombination of photogenerated electron-hole pairs [1, 31], resulting in unsatisfactory photocatalytic effect, which severely restricts its application in actual production. Therefore, how to improve the photocatalytic performance of g-C₃N₄, especially the excellent photocatalytic conversion and degradation nature under visible-light irradiation, has important theoretical and practical significance for the improvement of its comprehensive and practical application. Recently, developing porous g-C₃N₄ materials has been testified to be an effective approach for boosting the photocatalytic efficiency [32], because of not only enhancing the specific surface area and thus providing large number of catalytic active sites, but also facilitating the charge separation during the photocatalytic reactions [32-34].

In this work, g-C₃N₄ materials with porous structure and high specific surface area were obtained by one-step high-temperature calcination when ammonium

^{*}Address correspondence to these authors at the Anhui Key Laboratory of Spin Electron and Nanomaterials of Anhui Higher Education Institutes, School of Chemistry and Chemical Engineering, Suzhou University, Suzhou 234000, China; E-mail: xinyuanhappy2010@163.com, szxieyong@126.com

bicarbonate (NH_4HCO_3) was utilized as the gaseous template. The degradation effect of methylene blue (MB) dye under visible-light irradiation was investigated to explore the influence of this modification strategy on the photocatalytic performance. This work provides a feasible visible-light induced photocatalytic pathway for dye contamination treatment.

2. EXPERIMENTAL

2.1. Materials and Photocatalysts Synthesis

DCDA with purity of 98.0% and analytically purity level NH_4HCO_3 were both purchased from Sinopharm Chemical Reagent Co., Ltd, China.

The $\text{pg-C}_3\text{N}_4$ materials were synthesized with a facile gas template method. Firstly, a certain mass of DCDA, here fixed at 10 g, was mixed with various mass of NH_4HCO_3 thoroughly by grinding in an agate mortar, including DCDA: NH_4HCO_3 =5:1, 2.5:1 and 1:1 in mass ratio. The mixed raw materials placed in a quartz crucible and transferred to a muffle furnace were heated at a rate of $10\text{ }^\circ\text{C}/\text{min}$ to $550\text{ }^\circ\text{C}$ from the room temperature, and kept for 2 h at this temperature then cooling down to room temperature. The yellow product is finally ground in the agate mortar for further use. Meanwhile, the pure DCDA as the raw material was also calcined under the same conditions to produce the control material. The above photocatalyst materials were named as P0, P1, P2 and P3 with the content increment of NH_4HCO_3 in the DCDA- NH_4HCO_3 mixtures, i.e., 10:0, 10:2, 10:4 and 10:10 in mass ratio. The yields of the products were determined according to the mass fraction of the product in DCDA (10 g) raw material after calcination. The yield data were the average of at least three experiments. The schematic diagram of the synthesis procedure is shown in Figure 1.

2.2. Structure and Morphology Characterization

The structures of materials were analyzed on a SMARTLa Advance X-ray diffraction (XRD) diffractometer with $\text{CuK}\alpha$ radiation ($\lambda = 1.5147\text{ \AA}$) with the scanning rate and scope of $1\text{ }^\circ/\text{min}$ and $10\text{-}60^\circ$. The photocatalyst morphologies were inspected by using a Field Emission Scanning Electron Microscope (FESEM, SU1510, Hitachi).

2.3. Photocatalytic Activity

The effect of $\text{pg-C}_3\text{N}_4$ materials on photocatalytic degradation of MB dye was investigated under visible-light irradiation, and the digital image of the photocatalytic apparatus was displayed in Figure 2. In a typical reaction, photocatalytic degradation tests were carried out in a 150 mL glass container with an external temperature control function. The temperature of the dye solution was kept constantly at $25\text{ }^\circ\text{C}$. During the degradation test, the dye solution was always stirred with a magnetic stirrer. The visible-light source was supplied by a 300W Xenon lamp with a 420 nm cut-off filter. 120 mL of MB dye (16 mmol/L) and 1.0 g of grinding photocatalyst were added to the glass container. Before turn on the light, the mixture solution was stirred completely for 30 min at least to ensure that the adsorption of the dye on photocatalyst can reach saturation. 2 mL of dye solution sample was taken at a certain interval, and each experiment was repeated at least 3 times. The solution absorbance subjected to various degradation time after high-speed centrifugation was determined by a UV-vis spectrophotometer at 664 nm, and then the dye concentration was calculated according to concentration-absorbance standard curve of the solution. Eventually, the degradation rate was calculated according to formula 1.

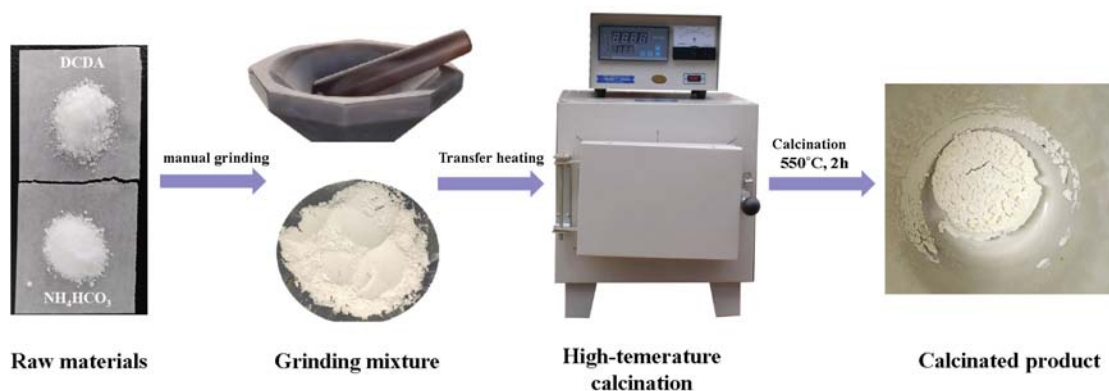


Figure 1: The schematic diagram of the synthesis procedure for the photocatalysts.

$$\eta = (1 - c_t/c_0) \times 100\% \quad (1)$$

Here, η was the degradation rate, and c_t was the solution concentration when the MB dye irradiated for time t , and c_0 was the initial solution concentration before test.

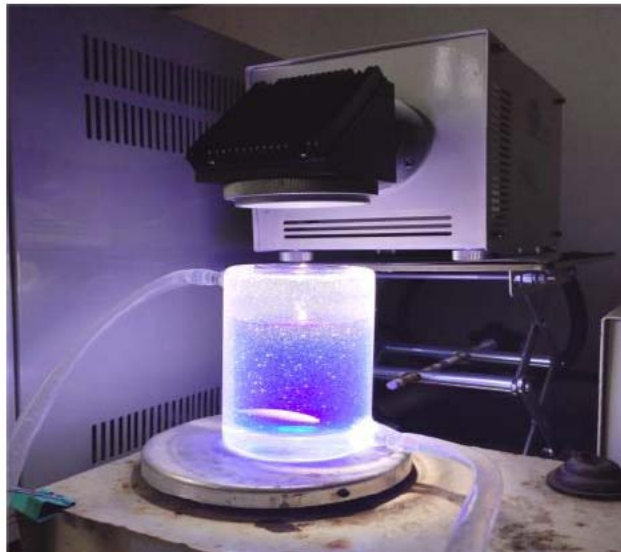


Figure 2: Digital photograph of the photocatalytic apparatus during the experiment.

3. RESULTS AND DISCUSSION

3.1. Characterization of pg-C₃N₄

The crystal and chemical structures of the synthesized materials were analyzed via the XRD, and the results are shown in Figure 3. It is observed that there are two obvious diffraction peaks located at 27.2° and 12.8° assigned to the (002) and (100) planes of g-C₃N₄ material [9, 10, 19-21], corresponding to the interlayer stacking for the π -conjugated layers [1, 9, 10, 26] with an interlayer distance of 0.33 nm and the in-plane repeating tri-s-triazine units [10, 30] with an interplanar spacing of 0.68 nm, respectively. These two typical peaks testify the generation of g-C₃N₄ materials. In addition, for the products calcined the mixtures of DCDA and NH₄HCO₃, i.e., P1-P3, other three diffraction peaks individually located at 19.6°, 22.0° and 25.2° appear on the XRD pattern, which can be attributed to the inter-planar size reduction and main structure destruction [35]. Moreover, it is obviously seen that the intensity of the above three diffraction peaks of the calcined products enhanced significantly with the content increment of NH₄HCO₃, which proved that the inter-planar size of the g-C₃N₄ materials further reduced, and macroscopically the micro-structures of the particle size became smaller. The above changes

of micro-structures and -morphologies are consistent with those observed by SEM below.

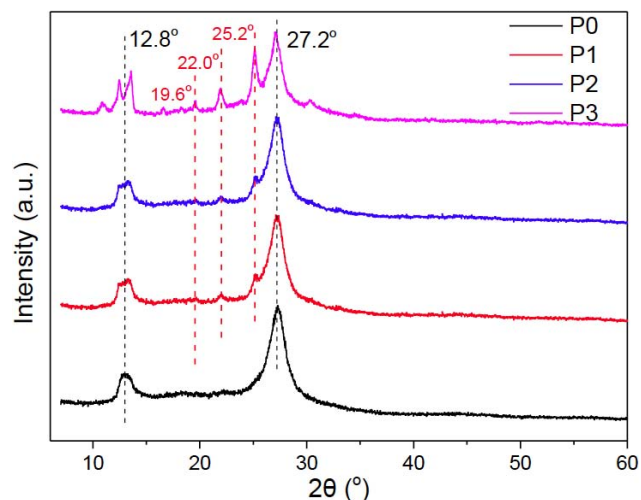


Figure 3: XRD patterns of various pg-C₃N₄ photocatalysts: P0-P3.

It is seen from Figures 4a1-a2 that the g-C₃N₄ itself can also present porous structures, which was ascribed to release of a small amount of NH₃ gas during the high-temperature calcination of DCDA [28]. By further comparing Figures 4b1-b2 and 4c1-c2 with 4a1-a2, it can be found that the obtained g-C₃N₄ materials behaved two changes in the micro-morphologies after calcining the mixture of DCDA and NH₄HCO₃. On the one hand, more particulate products at the micron scale were generated after adding NH₄HCO₃ into DCDA by carefully comparing Figures 4b1-b2 and 4c1-c2 with 4a1-a2. On the other hand, more micron porous structures were formed on the smaller particle surfaces. With the increasing amount of NH₄HCO₃ in the raw materials, the micro-structure changes of calcined products were more obvious in these two aspects potentially due to the heat-labile nature of NH₄HCO₃ and easier to fully decompose into CO₂, NH₃ and H₂O gases when heated. Therefore, the yields of the products also decreased with the increasing amount of NH₄HCO₃, as displayed in Figures 4d1-d2. In this case, it is anticipated and convinced that the change of the material microstructures and yields is bound to exert an important influence on its photocatalytic performance.

3.2. Photocatalytic Activity of pg-C₃N₄

Figure 5 gives the degradation rate curves of MB dye solution under visible-light irradiation with different pg-C₃N₄ photocatalysts (P1-P3), comparing with the control material (P0). As is seen from Figure 5, after 30 min of dark adsorption, using only DCDA calcined

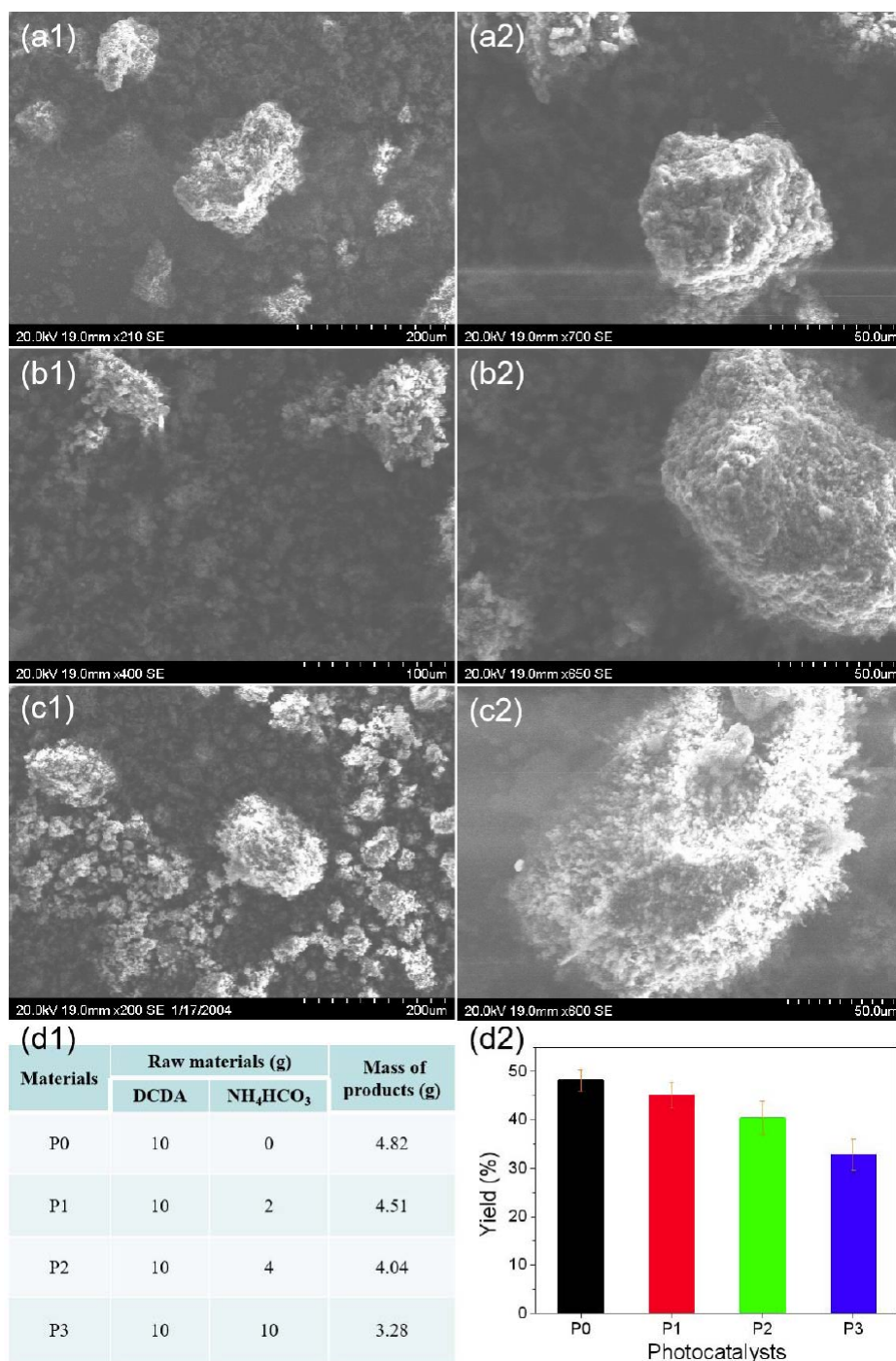


Figure 4: SEM micrographs with different magnifications of various g-C₃N₄ photocatalysts: P0 (a1, a2), P2 (b1, b2), P3 (c1, c2). Detailed information of synthesis process for the g-C₃N₄ photocatalysts (d1) and their yields (d2).

product (P0) as the photocatalyst, the MB dye solution can also be gradually degraded with the extension of light irradiation, and the degradation rate reached 36% at 2h and 71% at 3h, which fully certifies that g-C₃N₄ itself has a relatively excellent photocatalytic performance [10, 19], and this can also be reflected by the result without photocatalysts as shown in Figure 5. By mixing NH₄HCO₃ gaseous template into DCDA, the photocatalytic effect of calcined products, i.e., P1-P3, is

more remarkable under the same experimental conditions. Especially in the first 20 min, pg-C₃N₄ materials (P1-P3) exerted a rapid degradation and decolorization effect on MB dye. The degradation rate photocatalyzed by P1-P3 can reach more than 90% within 1.5 h, which is 6.5 times higher than that of P0 material. The degradation rate can come up to 99% within 2 h, and the complete degradation and decolorization of MB dyes are basically achieved. The

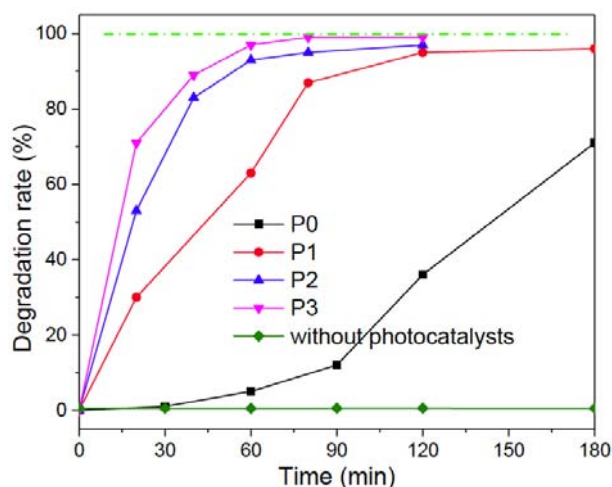


Figure 5: Degradation rates of MB dye catalyzed by the photocatalysts (P0-P3) for different time under visible-light irradiation.

underlying reasons for the outstanding photocatalytic performance of the pg-C₃N₄ materials, comparing with the control one, are potentially located that heat-labile NH₄HCO₃ decomposed into abundant of CO₂ and NH₃ gases, facilitating the destruction of the interlayer structures and formation of micro-scale porous structures, and correspondingly increasing the specific surface area, which greatly increased the contact area between the photocatalyst and the MB dye solution, and also exposed more active sites, thus improving the degradation effect of the dye solution under visible-light irradiation. Furthermore, in order to more intuitively show the degradation procedure of MB dye solution, Figure 6 provides the comparative digital photographs of MB dye solutions sampled at different irradiation time when using P1 as the photocatalyst.

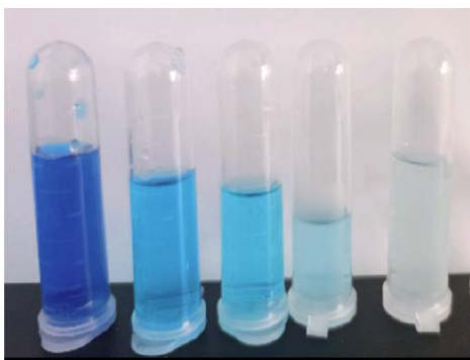


Figure 6: The digital photograph of the dye solution after degradation with different time. The samples from left to right were degraded for 0, 30, 60, 90, 120 min, respectively.

4. CONCLUSIONS

In the present work, pg-C₃N₄ materials were synthesized via a one-step high-temperature

calcination method using heat-labile NH₄HCO₃ as the gaseous template. The micro-structures and -morphologies of the porous materials were characterized by XRD and SEM respectively, and the photocatalytic degradation of MB dye was tested under visible-light irradiation. The following conclusions can be drawn:

1. g-C₃N₄ material was successfully synthesized via high-temperature calcination using DCDA as the raw material. More diffraction peaks appeared after mixing NH₄HCO₃ into DCDA after calcination, leading to inter-planar size reduction and main structure destruction of pg-C₃N₄, due to the heat-labile NH₄HCO₃ fully decomposing into CO₂, NH₃ and H₂O gases during heating.
2. Many smaller particulate products and more micro-scale porous structures formed on the smaller particle surfaces were generated after adding NH₄HCO₃ into DCDA, and the micro-structure changes of calcined products were more obvious with the increasing amount of NH₄HCO₃ in the raw materials, ascribing to its heat-labile nature and easier to decomposition. The products yields also decreased with the increasing amount of NH₄HCO₃.
3. As a photocatalyst, g-C₃N₄ itself can also behave a relatively excellent photocatalytic performance, the degradation rates of MB dye reaching 36% at 2h and 71% at 3h. The photocatalytic effect of calcined products of the mixtures was more remarkable. Particularly, the degradation rate photocatalyzed by pg-C₃N₄ materials can reach more than 90% within 1.5 h, which is 6.5 times higher than that of the control material. It comes up to 99% within 2 h, almost achieving the complete degradation and decolorization.

DECLARATION OF INTEREST STATEMENT

The authors state that there is no commercial or associative interest that represents a conflict of interest in connection with the present work.

DATA AVAILABILITY

Data will be made available on request.

ACKNOWLEDGEMENTS

The authors are grateful for the financial support from the Anhui Provincial Department of Education

Outstanding Youth Research Project (grant No. 2022AH020083), the Fund of Professor (Doctor) of Suzhou University Scientific Research Foundation Project (grant No. 2022BSK004), and the support of Applied Research Institute of Natural Products (grant No. 2021XJPT10ZC).

REFERENCES

- [1] Ong WJ, Tan LL, Ng YH, Yong ST, Chai SP. Graphitic carbon nitride (g-C₃N₄)-based photocatalysts for artificial photosynthesis and environmental remediation: Are we a step closer to achieving sustainability? *Chem Rev* 2016; 116: 7159-329. <https://doi.org/10.1021/acs.chemrev.6b00075>
- [2] Jiang W, Luo W, Wang J, Zhang M, Zhu Y. Enhancement of catalytic activity and oxidative ability for graphitic carbon nitride. *J Photoch Photobio C* 2016; 28: 87-115. <https://doi.org/10.1016/j.jphotochemrev.2016.06.001>
- [3] Deng L, Fang N, Wu S, Shu S, Chu Y, Guo J, et al. Uniform H-CdS@NiCoP core-shell nanosphere for highly efficient visible-light-driven photocatalytic H₂ evolution. *J Colloid Interface Sci* 2022; 608: 2730-9. <https://doi.org/10.1016/j.jcis.2021.10.190>
- [4] Mou Z, Meng T, Li J, Wang Y, Wang X, Guo H, et al. Significantly enhanced photocatalytic hydrogen production performance of MoS₂/CNTs/CdS with carbon nanotubes as the charge mediators. *Int J Hydrogen Energ* 2023. <https://doi.org/10.1016/j.ijhydene.2023.07.060>
- [5] Peng K, Zuo L, Wang Y, Ye J, Wang H, Jia Y, et al. Boosting photocatalytic hydrogen evolution over CdS/MoS₂ on the graphene/montmorillonite composites. *Appl Clay Sci* 2023; 236. <https://doi.org/10.1016/j.clay.2023.106855>
- [6] R S, Kavya krishnaveni T, Matheswaran M. Pyrolyzed synthesis of boron nitride for photocatalytic degradation of indigo carmine studies. *Opt Mater* 2023; 138. <https://doi.org/10.1016/j.optmat.2023.113719>
- [7] Sankeetha S, Muralidharan R, Abirami N, Leelavathi H, Tamizharasan S, Kumarasamy A, et al. Interaction of BiVO₄ anchored 2D hexagonal boron nitride nanocomposite for photocatalytic water pollutants degradation and phytotoxicity assessment. *Colloid Surfaces A* 2023; 675. <https://doi.org/10.1016/j.colsurfa.2023.132024>
- [8] Umadevi P, Ramya Devi KT, Sridevi DV, Perumal S, Ramesh V. Structural, morphological, optical, photocatalytic activity and bacterial growth inhibition of Nd-doped TiO₂ nanoparticles. *Mater Sci Eng B* 2022; 286: 116018. <https://doi.org/10.1016/j.mseb.2022.116018>
- [9] Wang H, Yuan X, Wang H, Chen X, Wu Z, Jiang L, et al. Facile synthesis of Sb₂S₃/ultrathin g-C₃N₄ sheets heterostructures embedded with g-C₃N₄ quantum dots with enhanced NIR-light photocatalytic performance. *Appl Catal B-Environ* 2016; 193: 36-46. <https://doi.org/10.1016/j.apcatb.2016.03.075>
- [10] Wang X, Maeda K, Thomas A, Takanabe K, Xin G, Carlsson JM, et al. A metal-free polymeric photocatalyst for hydrogen production from water under visible light. *Nat Mater* 2009; 8: 76-80. <https://doi.org/10.1038/nmat2317>
- [11] Fujishima A, Honda K. Electrochemical photolysis of water at a semiconductor electrode. *Nature* 1972; 238: 37-38. <https://doi.org/10.1038/238037a0>
- [12] Gao R, Xiong L, Huang L, Chen W, Li X, Liu X, et al. A new structure of Pt NF@Ni(OH)₂/CdS heterojunction: Preparation, characterization and properties in photocatalytic hydrogen generation. *Chem Eng J* 2022; 430: 132726. <https://doi.org/10.1016/j.cej.2021.132726>
- [13] Xue X, Dong W, Luan Q, Gao H, Wang G. Novel interfacial lateral electron migration pathway formed by constructing metallized CoP₂/CdS interface for excellent photocatalytic hydrogen production. *Appl Catal B-Environ* 2023; 334: 122860. <https://doi.org/10.1016/j.apcatb.2023.122860>
- [14] Oad N, Chandra P, Mohammad A, Tripathi B, Yoon T. MoS₂-based hetero-nanostructures for photocatalytic, photoelectrocatalytic and piezocatalytic remediation of hazardous pharmaceuticals. *J Environ Chem Eng* 2023; 11: 109604. <https://doi.org/10.1016/j.jece.2023.109604>
- [15] Xu Y, Ouyang J, Zhang L, Long H, Song Y, Cui Y. Embedded 1T-rich MoS₂ into C₃N₄ hollow microspheres for effective photocatalytic hydrogen production. *Chem Phys Lett* 2023; 814: 140331. <https://doi.org/10.1016/j.cplett.2023.140331>
- [16] Zhang J, Zan X, Shen X, Zheng H. Preparation of direct Z-scheme hierarchical MoS₂/MnO₂ composite for efficient adsorption and wide spectrum photocatalytic degradation of organic pollutants in water. *Mater Res Bull* 2023; 165: 112301. <https://doi.org/10.1016/j.materresbull.2023.112301>
- [17] Thi Huyen N, Van Tu N, Van Hau T, Van Trinh P, Thi Thanh C, Thu Loan N, et al. Boron nitride nanosheets decorated titanium dioxide nanorods for high photocatalytic degradation of methylene blue. *Mater Lett* 2023; 340: 134213. <https://doi.org/10.1016/j.matlet.2023.134213>
- [18] Yang C, Bu D, Huang S. Three-dimensional porous boron nitride with enriched defects and free radicals enables high photocatalytic activity for hydrogen evolution. *Chem Eng J* 2022; 446: 137026. <https://doi.org/10.1016/j.cej.2022.137026>
- [19] Niu P, Zhang L, Liu G, Cheng H-M. Graphene-like carbon nitride nanosheets for improved photocatalytic activities. *Adv Funct Mater* 2012; 22: 4763-70. <https://doi.org/10.1002/adfm.201200922>
- [20] Zhang L, Chen X, Guan J, Jiang Y, Hou T, Mu X. Facile synthesis of phosphorus doped graphitic carbon nitride polymers with enhanced visible-light photocatalytic activity. *Mater Res Bull* 2013; 48: 3485-91. <https://doi.org/10.1016/j.materresbull.2013.05.040>
- [21] Zhang L, Liu D, Guan J, Chen X, Guo X, Zhao F, et al. Metal-free g-C₃N₄ photocatalyst by sulfuric acid activation for selective aerobic oxidation of benzyl alcohol under visible light. *Mater Res Bull* 2014; 59: 84-92. <https://doi.org/10.1016/j.materresbull.2014.06.021>
- [22] Dai G, Xie J, Li C, Liu S. Flower-like Co₃O₄/graphitic carbon nitride nanocomposite based electrochemical sensor and its highly sensitive electrocatalysis of hydrazine. *J Alloy Compd* 2017; 727: 43-51. <https://doi.org/10.1016/j.jallcom.2017.08.100>
- [23] Chen Y, Zhang B, Liu Y, Chen J, Pan H, Sun W. Graphitic carbon nitride-based electrocatalysts for energy applications. *Mater Today Catal* 2023; 1: 100003. <https://doi.org/10.1016/j.mtcata.2023.100003>
- [24] Zhai H-S, Cao L, Xia X-H. Synthesis of graphitic carbon nitride through pyrolysis of melamine and its electrocatalysis for oxygen reduction reaction. *Chinese Chem Lett* 2013; 24: 103-6. <https://doi.org/10.1016/j.ccllet.2013.01.030>
- [25] Wu K, Ji J, Yang H, Zhou Z, Chen R, Liang S, et al. Multifunctional semiconducting carbon nitrides enabling sequential fluorescent sensing of telomerase activity and internal self-checking. *Sensor Actuat B-Chem* 2023; 378: 133170. <https://doi.org/10.1016/j.snb.2022.133170>
- [26] Zhao H-M, Sun T, Wang J, Xu A-J, Jia M-L, Xue B. Phosphorus-doped oligomeric carbon nitride for selective

- fluorescence detection of mercury (II) ions. *Dyes Pigments* 2022; 207: 110739.
<https://doi.org/10.1016/j.dyepig.2022.110739>
- [27] Lin X, Hong C, Lin Z, Huang Z. Rapid detection of histamine in fish based on the fluorescence characteristics of carbon nitride. *J Food Compos Anal* 2022; 112: 104659.
<https://doi.org/10.1016/j.jfca.2022.104659>
- [28] Wang Y, Wang X, Antonietti M. Polymeric graphitic carbon nitride as a heterogeneous organocatalyst: from photochemistry to multipurpose catalysis to sustainable chemistry. *Angew Chem Int Ed Engl* 2012; 51: 68-89.
<https://doi.org/10.1002/anie.201101182>
- [29] Zhao H, Yu H, Quan X, Chen S, Zhang Y, Zhao H, *et al.* Fabrication of atomic single layer graphitic-C₃N₄ and its high performance of photocatalytic disinfection under visible light irradiation. *Appl Catal B-Environ* 2014; 152-153: 46-50.
<https://doi.org/10.1016/j.apcatb.2014.01.023>
- [30] Chen X, Zhang L, Zhang B, Guo X, Mu X. Highly selective hydrogenation of furfural to furfuryl alcohol over Pt nanoparticles supported on g-C₃N₄ nanosheets catalysts in water. *Sci Rep* 2016; 6: 28558.
<https://doi.org/10.1038/srep28558>
- [31] Chen S, Hao N, Jiang D, Zhang X, Zhou Z, Zhang Y, *et al.* Graphitic carbon nitride quantum dots in situ coupling to Bi₂MoO₆ nanohybrids with enhanced charge transfer performance and photoelectrochemical detection of copper ion. *J Electroanal Chem* 2017; 787: 66-71.
<https://doi.org/10.1016/j.jelechem.2017.01.042>
- [32] Wang C, Fan H, Ren X, Fang J, Ma J, Zhao N. Porous graphitic carbon nitride nanosheets by pre-polymerization for enhanced photocatalysis. *Mater Charact* 2018; 139: 89-99.
<https://doi.org/10.1016/j.matchar.2018.02.036>
- [33] Wang K, Wang H, Cheng Q, Gao C, Wang G, Wu X. Molecular-functionalized engineering of porous carbon nitride nanosheets for wide-spectrum responsive solar fuel generation. *J Colloid Interf Sci* 2022; 607: 1061-70.
<https://doi.org/10.1016/j.jcis.2021.09.034>
- [34] Balakumar V, Ramalingam M, Sekar K, Chuaicham C, Sasaki K. Fabrication and characterization of carbon quantum dots decorated hollow porous graphitic carbon nitride through polyaniline for photocatalysis. *Chem Eng J* 2021; 426: 131739.
<https://doi.org/10.1016/j.cej.2021.131739>
- [35] Yan J, Rodrigues M-TF, Song Z, Li H, Xu H, Liu H, *et al.* Reversible formation of g-C₃N₄ 3D hydrogels through ionic liquid activation: Gelation behavior and room-temperature gas-sensing properties. *Adv Funct Mater* 2017; 27: 1700653.
<https://doi.org/10.1002/adfm.201700653>

Received on 15-06-2023

Accepted on 09-08-2023

Published on 17-08-2023

<https://doi.org/10.6000/1929-5995.2023.12.09>© 2023 Zhang *et al.*; Licensee Lifescience Global.

This is an open access article licensed under the terms of the Creative Commons Attribution License (<http://creativecommons.org/licenses/by/4.0/>) which permits unrestricted use, distribution and reproduction in any medium, provided the work is properly cited.